lubricants

MDPI

Article

Numerical Simulation of Startup Performance in High-Power Diesel Engine Lubrication Systems Under High-Altitude and Cold Conditions

Zhonghao Gao [1,†], Yiqiao Guo [1,†], Wendi Zhu [2], Wei Du [1,*], Lanjie Huang [3] and Hao Zhang [1,4,*]

[1] School of Mechanical Engineering, Beijing Institute of Technology, Beijing 100081, China; 3220240575@bit.edu.cn (Z.G.); 3120215268@bit.edu.cn (Y.G.)
[2] School of Automobile Engineering, Tianjin Transportation Technical College, Tianjin 300393, China; bit_zwd@163.com
[3] Hebei Huabei Diesel Engine Co., Ltd., Shijiazhuang 050081, China; hccpyfzx@chbdp.com
[4] Tangshan Research Institute, Beijing Institute of Technology, Tangshan 063000, China
* Correspondence: dwei@bit.edu.cn (W.D.); hao_zhang@bit.edu.cn (H.Z.)
† These authors contributed equally to this work.

Abstract

With the significant increase in the number of motor vehicles in plateau regions, the adaptability and reliability requirements of diesel engines operating under high-altitude and cold conditions have become increasingly critical. In this study, a one-dimensional transient simulation model of the overall engine lubrication system was developed based on a physical experimental prototype. The multiphysics-coupled lubrication system was numerically modeled and analyzed, with particular emphasis on elucidating the influence mechanisms of high-altitude and cold environments on the startup performance of diesel engine lubrication systems. System responses under different ambient pressures (0.88 bar, 0.92 bar, 0.96 bar, and standard atmospheric pressure) and oil temperatures (30 °C, 55 °C, and 100 °C) were systematically investigated. In addition, variations in the opening degree of the oil pump pressure relief valve (closed, 4%, 30%, 60%, and 100%) were incorporated to reveal the governing effects of high-altitude and cold environments on lubrication system startup behavior. The results indicate that under high-altitude and cold conditions, the decrease in oil temperature is the dominant factor and exerts the most significant influence on the steady-state oil pressure and flow rate of the lubrication system. Variations in ambient pressure lead only to an equivalent shift in absolute oil pressure, with negligible effects on relative oil pressure, steady-state flow rate, response time, or filling rate. However, a reduction in atmospheric pressure leads to a decrease in the peak oil flow rate at the outlet of the oil pump. The opening degree of the pressure relief valve exhibits a nonlinear influence on the startup performance of the lubrication system, and significantly decreases the oil filling rate. This study innovatively develops a lubrication system performance prediction model under high-altitude, low-pressure, and low-temperature conditions. Calibrated using vehicle road-test data, the model quantifies for the first time the relative contributions of the three key factors to start-up lubrication performance, thereby providing a clear decision-making framework and prioritized improvement directions for the reliability-oriented design and safety threshold calibration of lubrication systems in high-altitude diesel engines.

Keywords: high-altitude and cold environment; diesel engine lubrication system; transient startup; lubrication

Check for updates

Received: 7 January 2026
Revised: 29 January 2026
Accepted: 10 February 2026
Published: 12 February 2026

Copyright: © 2026 by the authors. Licensee MDPI, Basel, Switzerland. This article is an open access article distributed under the terms and conditions of the Creative Commons Attribution (CC BY) license.

1. Introduction

Plateau regions are characterized by thin air, low atmospheric pressure, and large diurnal temperature variations; consequently, plateau atmospheric conditions exert a significant influence on the performance of diesel engines [1–3]. Under high-altitude and cold environments, increased oil viscosity leads to higher resistance during the engine startup process. As the lubrication system serves as the core guarantee for the efficient operation of diesel engine friction pairs, it directly determines the overall mechanical efficiency and service life of the engine [4,5]. Therefore, against the dual background of global energy conservation and emission reduction, as well as the rapid increase in vehicle ownership in plateau regions [6,7], investigating the effects of high-altitude and cold environments on the startup performance of engine lubrication systems constitutes a critical step toward improving engine altitude adaptability and operational reliability. To predict these effects, a considerable number of theoretical analyses and experimental studies have been conducted both domestically and internationally.

Zhang et al. [8] conducted experimental and simulation-based validation using a test bench and performed transient analyses of the engine cold-start process. Their results showed that extending the start-up duration effectively reduces the average dry-sliding velocity of bearings, thereby significantly decreasing friction and wear of critical friction pairs during start-up. Chen et al. [9] developed a transient mixed lubrication model to predict the time-dependent wear behavior of main bearings under dynamic loading conditions and systematically investigated the influence of engine start-up on main bearing lubrication and wear characteristics. The results indicated that the wear rate of the main bearings gradually stabilizes with increasing numbers of start-up cycles, and that the effect of start-up duration on bearing wear is significantly more pronounced than that of radial clearance. Celik et al. [10] explored the influence of a vortex tube on the cold-start performance of diesel engines through full-engine experiments, demonstrating that the vortex tube improves cold-start performance by increasing intake air temperature, shortening start-up duration, and reducing fuel consumption. Yang et al. [11] investigated the cold-start performance of high-pressure common-rail hybrid diesel engines and found that under extreme plateau conditions, diesel engines tend to experience incomplete combustion. This phenomenon leads to dilution of the lubricant by unburned fuel, thereby reducing the overall lubrication performance of the system. Lu et al. [12], through computational fluid dynamics (CFD) analysis of the dynamic response parameters of steam relief valves, pointed out that optimizing fuel injection strategies can shorten engine start-up time, enabling faster oil filling within the lubrication system and reducing the duration of boundary lubrication. Liu et al. [13] conducted experiments to identify the fundamental causes of diesel engine performance degradation in plateau regions, concluding that the increased thermal load on the lubrication system arises from reduced combustion and thermal efficiency in high-altitude environments.

Zare et al. [14] conducted customized cold-start tests on diesel engines to investigate lubrication oil particulate emissions and engine performance during cold-start and hot-running phases. Their findings revealed a strong correlation between increasing engine temperature and enlarged lubricant particle size during cold start, whereas during hot operation, further temperature increases were closely associated with a reduction in particle size. He et al. [15] simulated the emission characteristics of heavy-duty diesel engines under plateau conditions and reported that combustion deterioration and accelerated lubricant degradation at high altitudes indirectly impair the lubrication performance of the system. Ceballos et al. [16] examined the effects of plateau environments on the performance of naturally aspirated engines, highlighting that the lubrication system is strongly affected by increased thermal load and viscosity variations in the lubricant. Qi et al. [17], using

a portable emission measurement system, analyzed vehicle emission variations under plateau conditions and found that engine thermal management becomes more challenging and the lubrication system experiences increased load. Liu et al. [18] developed a cylinder liner–piston ring wear simulation model and demonstrated through simulations that rising altitude leads to higher engine thermal loads and reduced oil viscosity. They suggested that the lubrication system must adapt to the thermomechanical coupling characteristics of high-altitude environments to prevent aggravated wear. Tobar et al. [19] investigated the performance of lubricants with different viscosities under high-load conditions, showing that high-viscosity oils can increase CO_2 emissions at high altitudes and heavy loads. They recommended developing new lubricant formulations tailored for low-pressure, low-oxygen plateau environments, achieving a balance between low-temperature fluidity and high-temperature oxidation resistance.

In previous studies on engine low-temperature start, research efforts have primarily focused on the effects of different low-temperature start strategies on critical engine friction pairs, whereas investigations into the influence of high-altitude environments on low-temperature start characteristics remain relatively limited. Moreover, most studies addressing engine operation under high-altitude conditions have inferred the effects of altitude on the thermal load and material composition of lubricating oil indirectly through analyses of combustion processes and emission characteristics, and subsequently discussed the overall impact on the lubrication system. However, such indirect approaches exhibit inherent limitations in terms of comprehensiveness and accuracy, making it difficult to elucidate the direct mechanisms by which high-altitude environments affect the engine's low-temperature start process. In contrast to these prior approaches, the present study directly investigates the startup process of a diesel engine lubrication system under high-altitude and cold conditions. A system-level one-dimensional transient simulation model was developed based on a physical experimental prototype, aiming to elucidate the direct effects of low pressure and low temperature in plateau environments on the startup performance of the lubrication system. By setting the gradient variations of atmospheric pressure and oil temperature, the study systematically analyzes their influence on the startup behavior of the lubrication system.

During the startup experiments of diesel engines conducted under high-altitude and low-temperature conditions, severe lubrication failures were observed, accompanied by instances where the pressure sensors installed along the oil galleries registered no readings. It is hypothesized that this phenomenon may be related to wear or malfunction of the oil pump relief valve. Under high-altitude and low-temperature conditions, reduced ambient pressure and low temperature may cause the actual relief pressure of the valve to fall below its design value and alter the reference pressure differential, ultimately resulting in a larger actual opening of the relief valve and premature pressure relief [20–22].

Based on these observations, this study considers oil temperature, atmospheric pressure, and the opening of the oil pump relief valve as key variables. The lubrication performance during the startup process under high-altitude and cold conditions is comprehensively evaluated from four perspectives: transient oil pressure curve, transient oil flow rate curve, oil film thickness, and pressure of each main bearing and the transient oil filling process within the lubrication system. By analyzing these simulation results, the study reveals the influence mechanisms of high-altitude and low-temperature environments on the startup performance of diesel engine lubrication systems.

2. Simulation Model

In this study, the lubrication system of a high-power V8 diesel engine was selected as the research object, and its specific structure is illustrated in Figure 1. The lubrication

system is driven by an oil pump and delivers lubricating oil through the pressurized oil circuit to key friction pairs such as the crankshaft, camshaft, and piston/cylinder liner assemblies. The system performs essential functions, including friction reduction, cooling, cleaning, sealing, and corrosion prevention. During operation, the lubricating oil circulates sequentially through the oil sump, oil pump, oil cooler, oil filter, and various friction pairs, before returning to the oil sump, thus forming a complete closed-loop circuit.

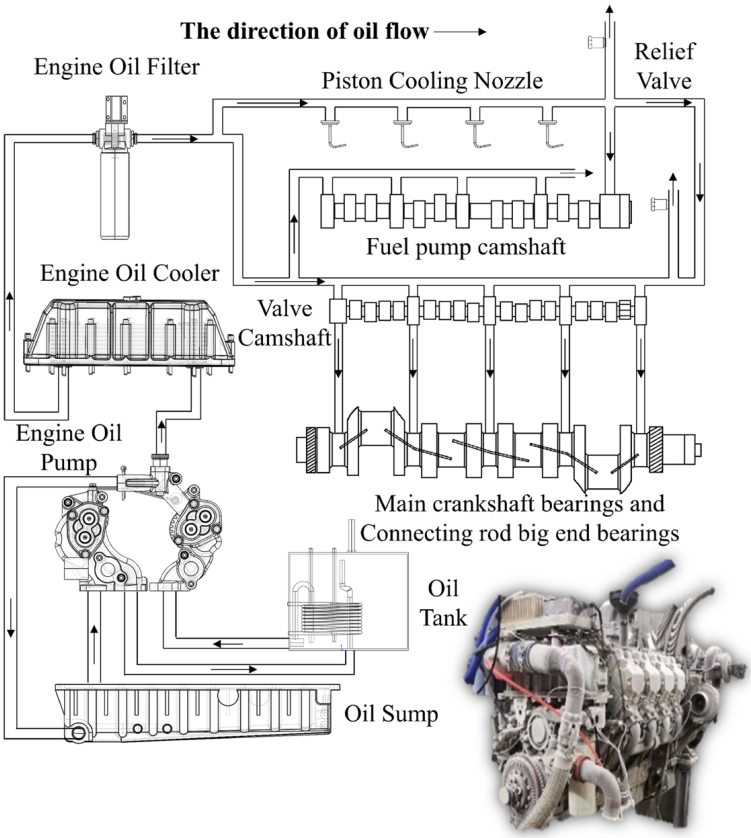


Figure 1. Structural diagram of the lubrication system of a specific high-power V8 diesel engine.

In this study, a system-level one-dimensional transient simulation model of the diesel engine lubrication system was established using GT-Suite, as illustrated in Figure 2. The three-dimensional lubrication system pipelines were equivalently reduced to a one-dimensional oil circuit model through the GEM-3D module in GT-Suite, followed by discretization using computational grids. Based on the compressible one-dimensional Navier–Stokes equations, including the continuity, momentum, and energy equations [23–25], the model employs a fully implicit SIMPLE algorithm to couple pressure, flow rate, and temperature within a maximum time step of 1 ms, thereby enabling efficient simulation of the startup process of the diesel engine lubrication system.

During transient startup simulations, the model simultaneously solves all conservation equations while incorporating nonlinear phenomena such as oil pump speed fluctuations and transient bearing clearances. Additionally, it accounts for wall thermal inertia and the dynamic variation of the oil film clearance, thereby improving the accuracy of the transient response prediction of the lubrication system under the startup process.

Considering that the flow resistance at various nodes within the lubrication system significantly influences the dynamic oil filling behavior [26,27], this study further refines the accuracy of simulating the oil filling process during engine startup by modeling and parameterizing key components of the lubrication system. These components include the oil pump, oil cooler, oil filter, main crankshaft bearings, connecting rod big end bearings, valve

camshaft bearings, fuel pump camshaft bearings, and piston cooling nozzle. As illustrated in Figure 2, the main bearings are sequentially numbered from one to six in the order of decreasing proximity to the oil pump. Moreover, the local flow resistances generated by structures such as the piston rings, piston skirt, and cylinder liner are equivalently integrated as additional flow resistances within the piston cooling nozzle module, thereby ensuring a comprehensive characterization of the overall flow characteristics of the system.

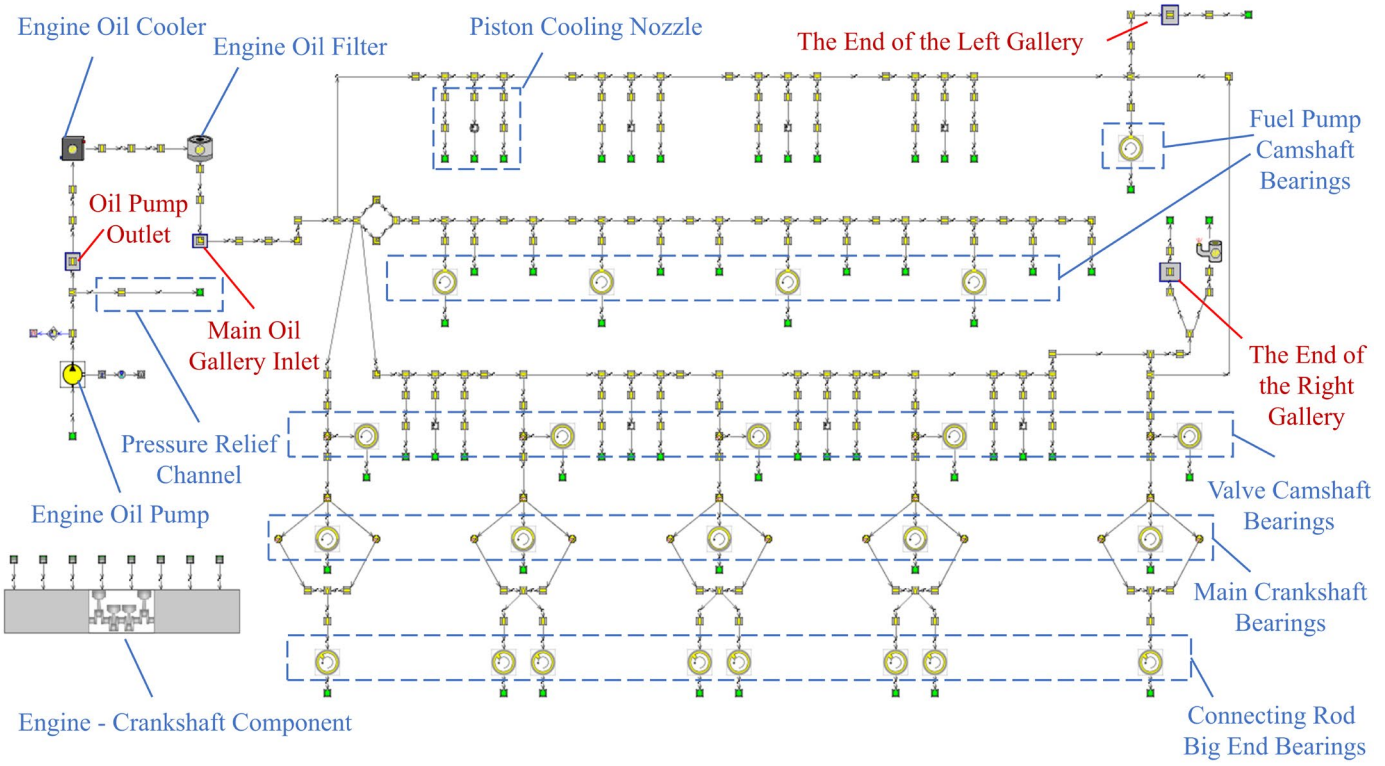


Figure 2. One-dimensional simulation model for the lubrication system of a specific high-power V8 diesel engine.

The fluid dynamic characteristics of the oil filter, oil cooler, and piston cooling nozzles were incorporated into the transient simulation model in the form of oil flow rate–pressure drop resistance curves. The dynamic response of the lubrication system during the startup process was driven in real time by the coupled engine–crankcase assembly, with the in-cylinder pressure curve (as shown in Figure 3) used as the boundary condition. By applying this curve as a dynamic input, a full-cycle numerical solution of the transient dynamics of the lubrication system during startup could be achieved. The opening degree of the oil pump relief valve was controlled by the diameter of the relief channel, and the relationship between the channel diameter and the relief valve opening is summarized in Table 1.

Table 1. The relationship between pipe diameter and the opening degree of the pressure relief valve.

The Opening Degree of the Pressure Relief Valve (%)	Pressure Relief Channel Diameter (mm)
0	No Channel
4	1.8
30	4.93
60	6.97
100	9

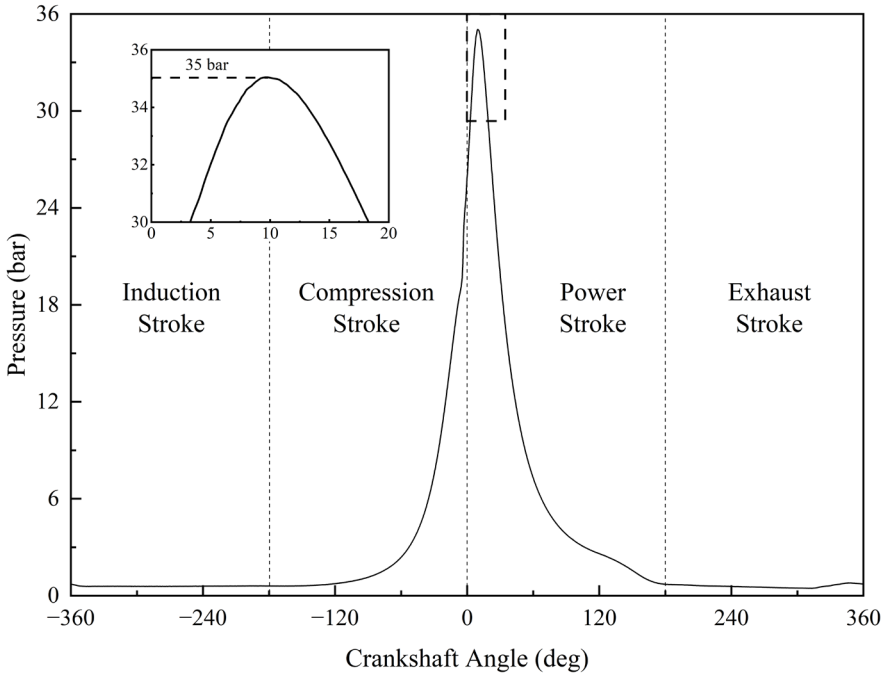


Figure 3. The curve of cylinder pressure with crankshaft angle at 600 rpm condition.

The engine oil used in this study was of grade 15W40. The primary flow resistance components in the lubrication system are the bearing elements. A parametric modeling approach was adopted to achieve coupled modeling between the bearing components and the engine–crankcase dynamic system, enabling accurate calculation of the fluid resistance characteristics within the bearing regions.

In the model, the oil pump component determines the oil flow rate and pressure rise during the startup process by interpolating a measured rotational speed–oil flow–oil pressure rise MAP. It should be noted that the oil pressure rise refers to the pressure increase generated by the oil pump rather than the absolute system pressure. The MAP was obtained from experimental measurements of the prototype engine, and the engine input speed profile applied in the simulation is shown in Figure 4.

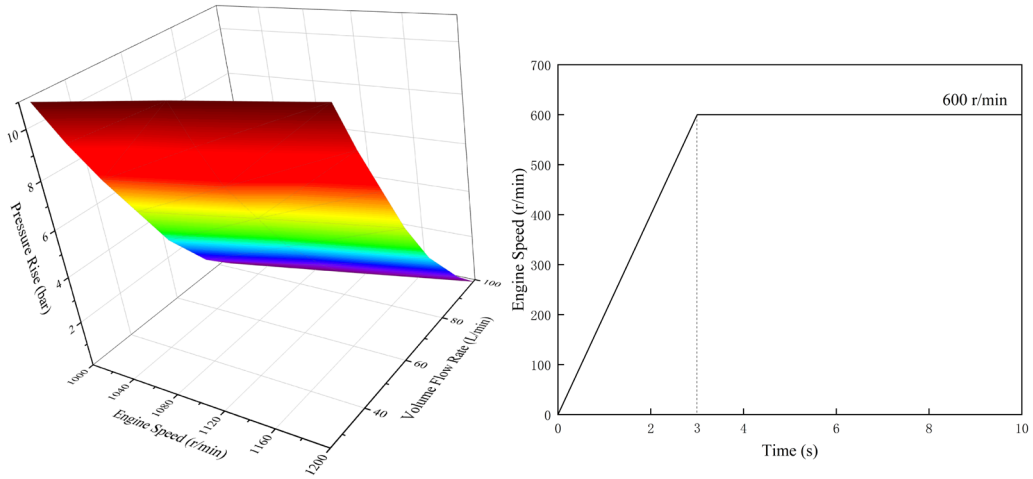


Figure 4. MAP of engine oil pump flow rate, pressure rise, and rotational speed, along with the input rotational speed curve.

In the lubrication system of the diesel engine, the oil pump is mechanically driven by a gear located at the free end of the crankshaft within the crankcase. The rotational speed ratio between the oil pump and the crankshaft is 1.68:1.

The model employed in this study is highly similar to that used by Guo et al. [28] in their investigation of cold-start pre-lubrication of diesel engine lubrication systems, which provides a certain level of confidence in its reliability. In addition, the accuracy of the model is validated using vehicle test data obtained from a high-altitude dedicated proving ground. Owing to the technical difficulties associated with installing external pressure sensors under on-vehicle testing conditions, the pressure sensor originally equipped at the downstream end of the left main oil gallery is used for data comparison. The specific calibration conditions and accuracy assessment are presented in Table 2.

Table 2. Calibration conditions and accuracy of the model.

Oil Temperature (°C)	Atmospheric Pressure (Bar)	Relief Valve Opening Degree (%)	Test Oil Pressure (Bar)	Simulated Oil Pressure (Bar)	Accuracy (%)
30	0.88	4	1.65	1.59	96.36

For uncertainty assessment of the proposed model, a preliminary evaluation was conducted using the parameter range perturbation method. Pipeline friction loss and pump efficiency were selected as key parameters, and three operating scenarios were defined: baseline, worst-case, and best-case conditions. The results indicate that the model provides reasonable credibility in predicting system-level trends; however, limitations remain in the prediction of absolute values. Therefore, it is recommended that engineers apply the conclusions of this study using conservative design margins that account for tolerance variations specific to the target engine platform.

3. Simulation Results and Discussion

To systematically investigate the influence mechanisms of ambient pressure and oil temperature on the startup performance of a diesel engine lubrication system under high-altitude and cold conditions, three sets of variables were introduced to examine the parametric gradient effects. First, in high-altitude environments, the oil temperature of an engine typically remains no lower than 20–30 °C after shutdown, owing to the thermal inertia of the cylinder block. Therefore, with the oil temperature fixed at 30 °C and the pressure relief valve opening set to 4%, the ambient pressure was varied across four levels: 1.00 bar, 0.96 bar, 0.92 bar, and 0.88 bar. Second, with the ambient pressure fixed at 0.88 bar and the pressure relief valve opening maintained at 4%, the oil temperature was varied at 30 °C, 55 °C, and 100 °C. Third, with the oil temperature fixed at 30 °C and the ambient pressure fixed at 0.88 bar, the pressure relief valve opening was varied at 4%, 30%, 60%, 100%, and the fully closed condition.

To evaluate the overall startup performance of the lubrication system, four key locations were selected as observation points: the oil pump outlet, the main oil gallery inlet, and the ends of the left and right galleries, as illustrated in Figure 2. By analyzing the simulated data at these locations, the direct effects of high-altitude and cold environments on the startup process of the diesel engine lubrication system were quantitatively revealed.

3.1. Influence of Atmospheric Pressure on the Startup Performance of Lubrication Systems

Under different ambient pressure conditions, the transient oil pressure curves at the oil pump outlet, the inlet of the main oil gallery, and the downstream ends of the left and right main oil galleries are shown in Figure 5. It should be noted that the pressures presented in Figure 5 are absolute oil pressures. As illustrated in Figure 5, with increasing altitude, the steady-state oil pressure at all monitored locations exhibits a monotonic decreasing trend. When the ambient pressure decreases from 1.00 bar to 0.88 bar, the steady-state absolute

oil pressure at the oil pump outlet decreases from 2.19 bar to 2.06 bar, corresponding to a reduction of approximately 5.9%. Similarly, the steady-state absolute oil pressure at the inlet of the main oil gallery decreases from 1.78 bar to 1.66 bar, with a reduction of approximately 6.7%. The steady-state absolute oil pressures at the downstream ends of both the left and right main oil galleries decrease from 1.71 bar to 1.59 bar, representing a reduction of approximately 7.0%.

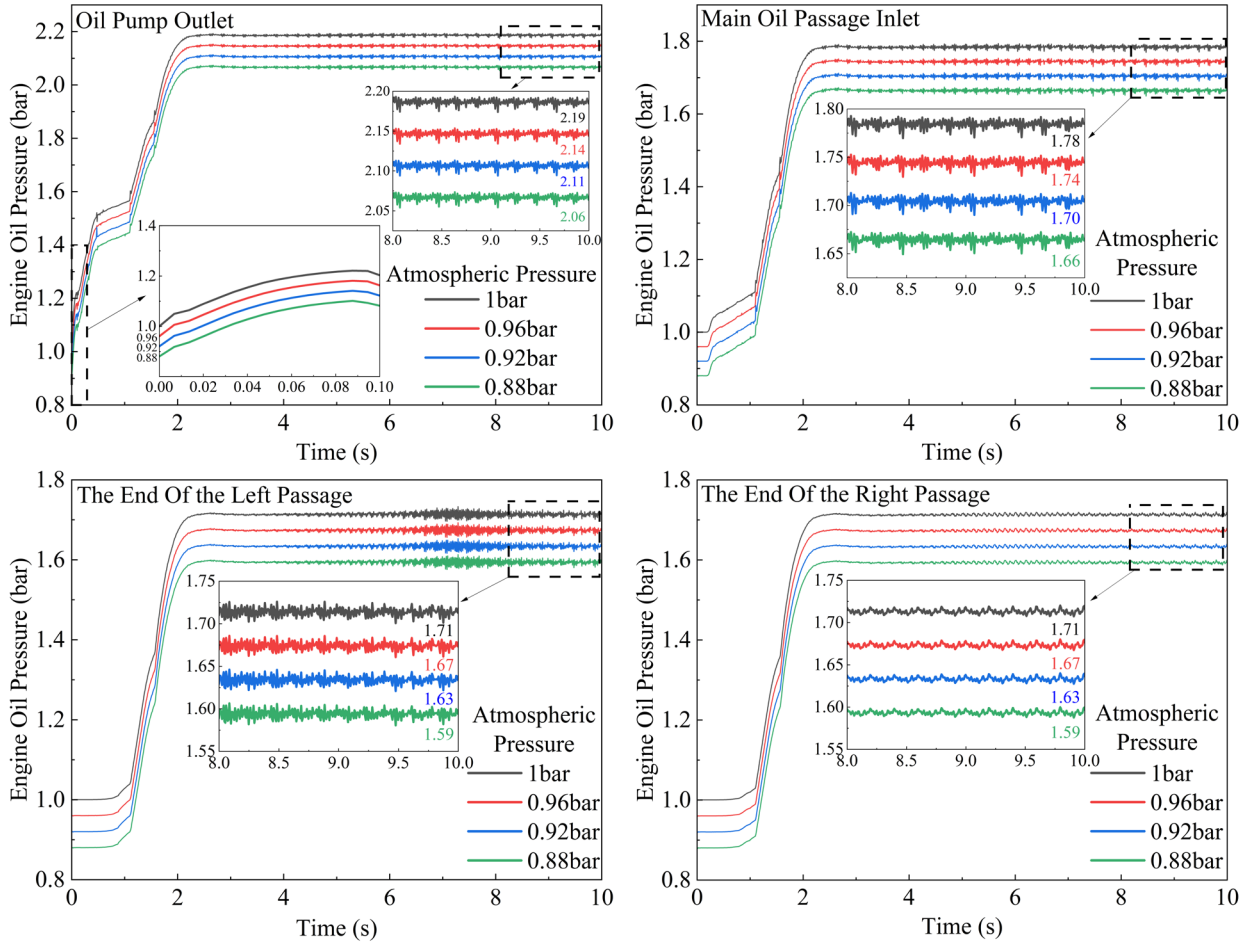


Figure 5. The influence of different altitude levels on the oil pressure of each node.

However, when the ambient pressure decreases from 1.00 bar to 0.88 bar, no noticeable variation is observed in the relative oil pressure at the key locations. Specifically, the steady-state relative oil pressure at the oil pump outlet remains at approximately 1.19 bar, while that at the inlet of the main oil gallery and at the downstream ends of the left and right main oil galleries remains at approximately 0.78 bar and 0.71 bar, respectively. These results indicate that a reduction in ambient pressure leads to an overall downward shift in the absolute oil pressure level of the lubrication system, whereas its relative pressure distribution remains essentially unchanged. In addition, ambient pressure exerts no significant influence on the rate at which the absolute oil pressure reaches steady state during the cold-start process, with the oil pressure at all key locations stabilizing at approximately 2.2 s.

Figure 6 presents the transient oil flow rate curves at the oil pump outlet, the inlet of the main oil gallery, and the downstream ends of the left and right main oil galleries under different ambient pressure conditions. When the ambient pressure decreases from 1.00 bar to 0.88 bar, no significant variation is observed in the steady-state oil flow rate. However, the peak oil flow rate at the oil pump outlet exhibits a slight reduction with decreasing ambient pressure, decreasing from 79.62 L/min to 60.12 L/min, corresponding

to a reduction of approximately 24.5%. In contrast, no obvious changes are observed in the peak oil flow rates at the inlet of the main oil gallery or at the downstream ends of the left and right main oil galleries.

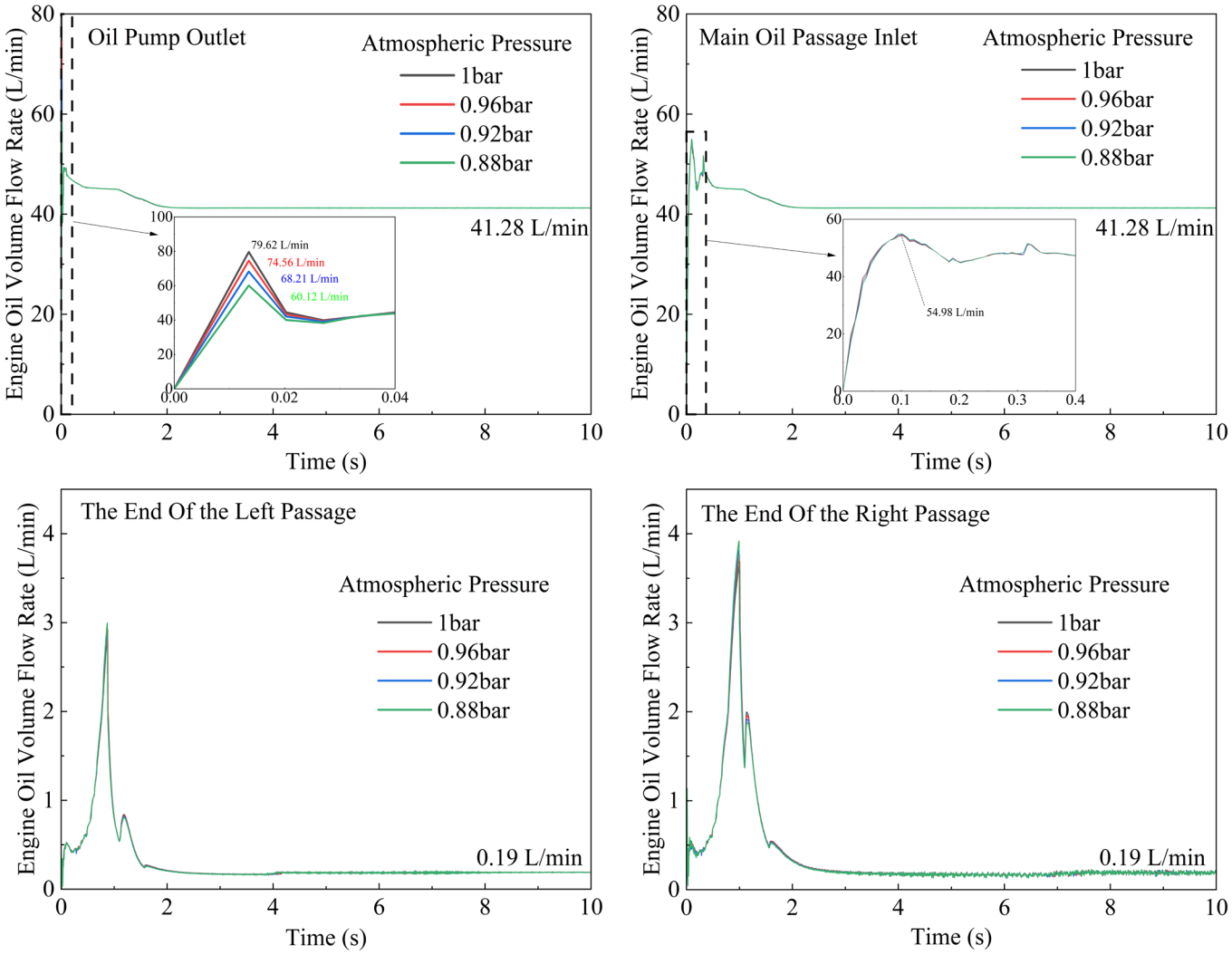


Figure 6. The influence of different altitude levels on the oil volume flow rate of each node.

Overall, variations in ambient pressure have a negligible effect on the steady-state oil flow rate during the startup process of the lubrication system and only result in a moderate reduction in the peak oil flow rate at the oil pump outlet.

Figure 7 presents the oil filling status of the lubrication system at 2 s of the engine startup at various atmospheric pressures. Ambient pressure has no discernible effect on the oil filling rate of the lubrication system during the startup process. Furthermore, under all ambient pressure conditions, the final result indicates the oil reaches and fills the last crankshaft main bearing at approximately 9.7 s.

Figure 8 presents the calculated minimum steady-state oil film thickness and maximum steady-state oil film pressure for each main bearing under different ambient pressure conditions. The results indicate that the minimum steady-state oil film thickness of the main bearings is approximately 10 μm, while the maximum steady-state oil film pressure is about 250 MPa. As ambient pressure varies, no pronounced changes are observed in the lubrication performance parameters of the crankshaft main bearings. These findings suggest that a reduction in ambient pressure has no significant influence on the bearing lubrication state and is insufficient to directly exacerbate bearing wear.

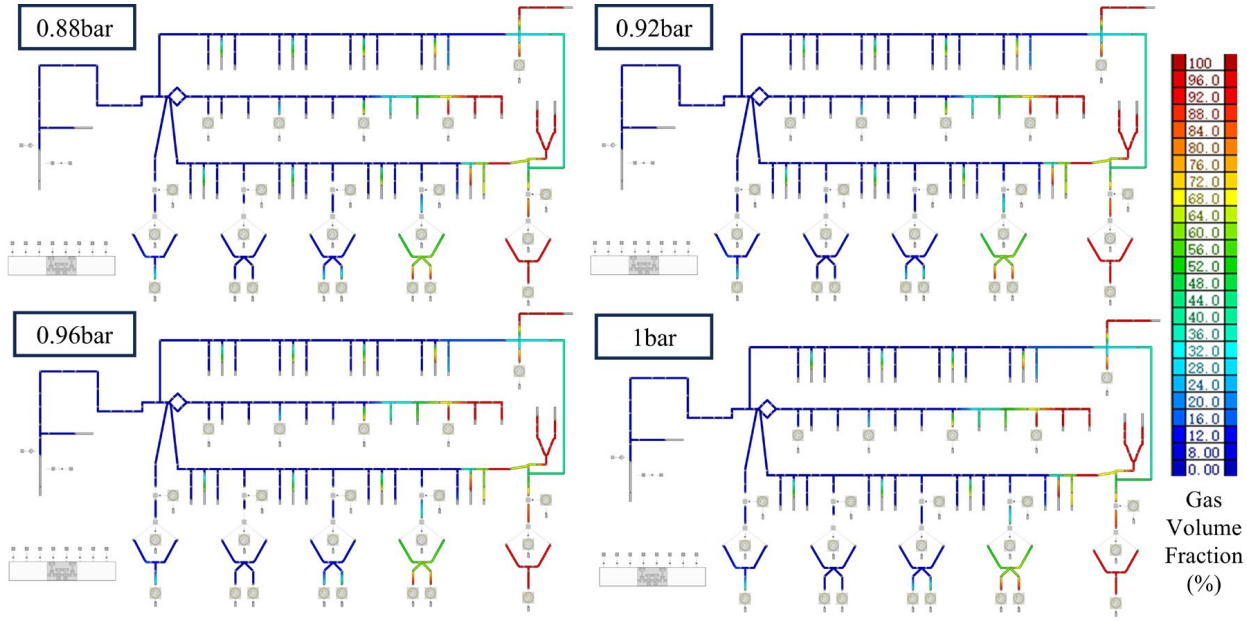


Figure 7. Oil filling status of the lubrication system at 2 s of the engine startup at various atmospheric pressures.

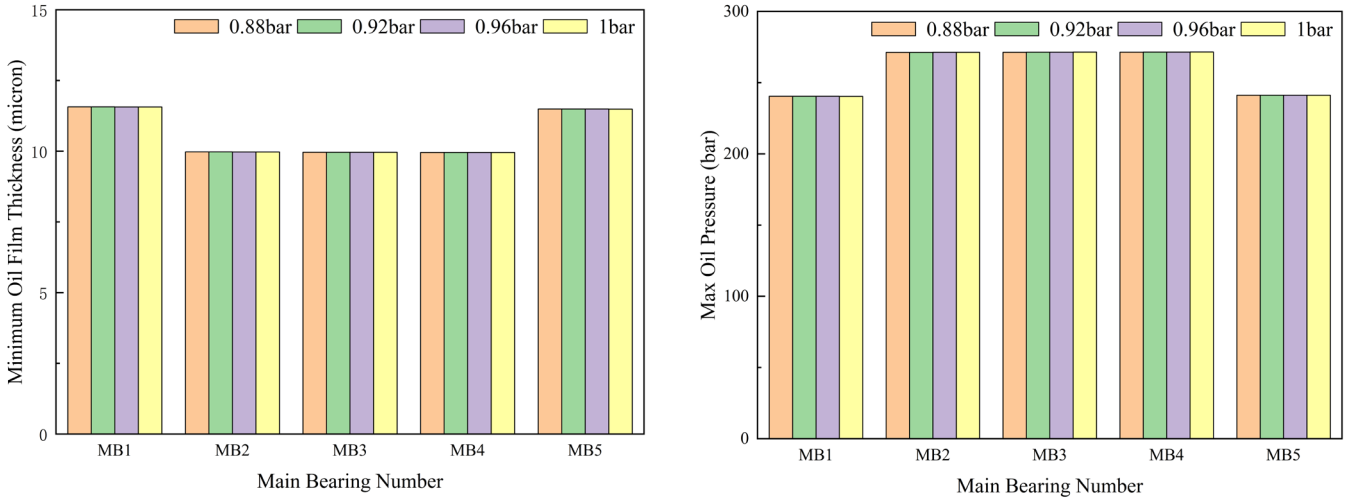


Figure 8. The lubrication status of each bearing: (**a**) maximum steady-state oil film pressure of each main bearing under different atmospheric pressure conditions; (**b**) minimum steady-state oil film thickness of each main bearing under different atmospheric pressure conditions.

3.2. Influence of Oil Temperature on the Startup Performance of Lubrication Systems

Figure 9 presents the transient oil pressure curves at the oil pump outlet, the inlet of the main oil gallery, and the downstream ends of the left and right main oil galleries under an ambient pressure of 0.88 bar for three oil temperature conditions (30 °C, 55 °C, and 100 °C). When the oil temperature decreases from 100 °C to 30 °C, the steady-state oil pressure at the oil pump outlet increases from 1.40 bar to 2.07 bar, corresponding to an increase of approximately 47.9%. Similarly, the steady-state oil pressure at the inlet of the main oil gallery increases from 1.09 bar to 1.66 bar, representing an increase of approximately 52.3%. This behavior can be attributed to the increase in oil viscosity at lower temperatures, which reduces system leakage and enhances the volumetric efficiency of the oil pump [29]. Meanwhile, the increased oil viscosity improves the load-carrying capacity of the oil pump and strengthens the throttling effect of leakage paths across the clearances of friction pairs,

leading to an overall rise in the system pressure level [30]. As indicated in Figure 8, under the 30 °C condition, a pronounced delay is observed in the oil pressure build-up process: the oil pressure at the oil pump outlet reaches its steady-state value at approximately 2.2 s, whereas only 1.9 s is required under the 100 °C condition. The oil pressure at the inlet of the main oil gallery exhibits a similar trend.

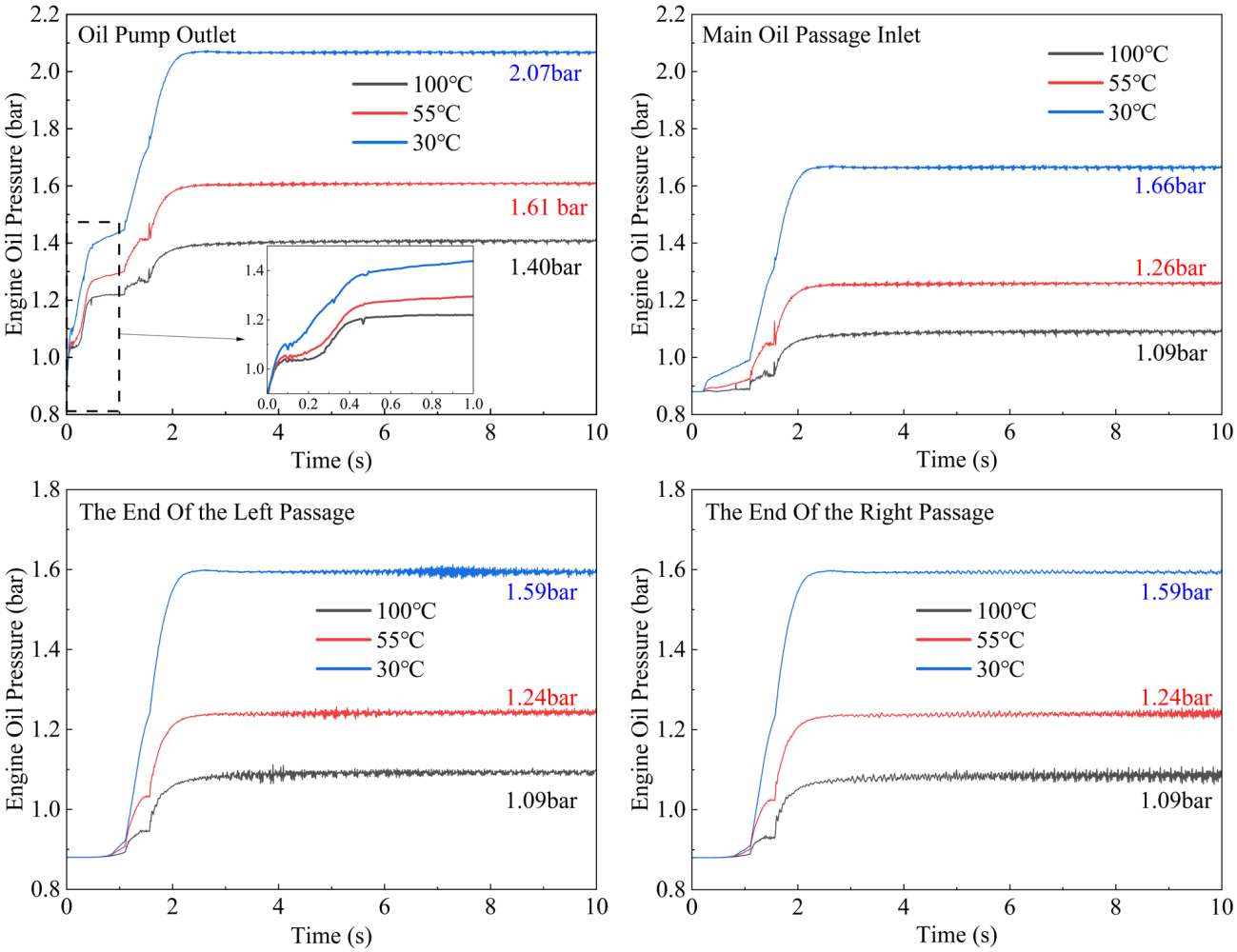


Figure 9. The influence of different oil temperatures on the oil pressure at each node.

Figure 10 illustrates the transient oil flow rate curves at the oil pump outlet, the inlet of the main oil gallery, and the downstream ends of the left and right main oil galleries under an ambient pressure of 0.88 bar for three oil temperature conditions (30 °C, 55 °C, and 100 °C). As shown in Figure 9, when the oil temperature decreases from 100 °C to 30 °C, the steady-state oil flow rates at both the oil pump outlet and the inlet of the main oil gallery decrease from 44.6 L/min to 41.2 L/min, corresponding to a reduction of approximately 7.6%. However, at the initial stage of the startup process, a pronounced decrease is observed in the peak oil flow rate at the oil pump outlet, which drops from 214.31 L/min to 60.12 L/min, representing a reduction of approximately 71.9%, whereas the peak oil flow rate at the inlet of the main oil gallery shows no significant variation. These results indicate that a decrease in oil temperature has a substantial impact on the peak oil flow rate at the oil pump outlet during the startup transient.

Moreover, a reduction in oil temperature delays the response time required for the oil flow rate to reach steady state. Under the 30 °C condition, the oil flow rate at the oil pump outlet reaches its steady-state value at approximately 2.1 s, whereas only 1.8 s is required under the 100 °C condition. A similar trend is observed at the inlet of the

main oil gallery, where the time required to reach steady state increases by approximately 16.7%. This behavior can be attributed to the higher inertia and increased flow resistance of low-temperature, high-viscosity oil, which prolongs the oil filling process of the lubrication system during cold start. In contrast, high-temperature, low-viscosity oil exhibits lower flow resistance, resulting in a faster transient response during the startup process.

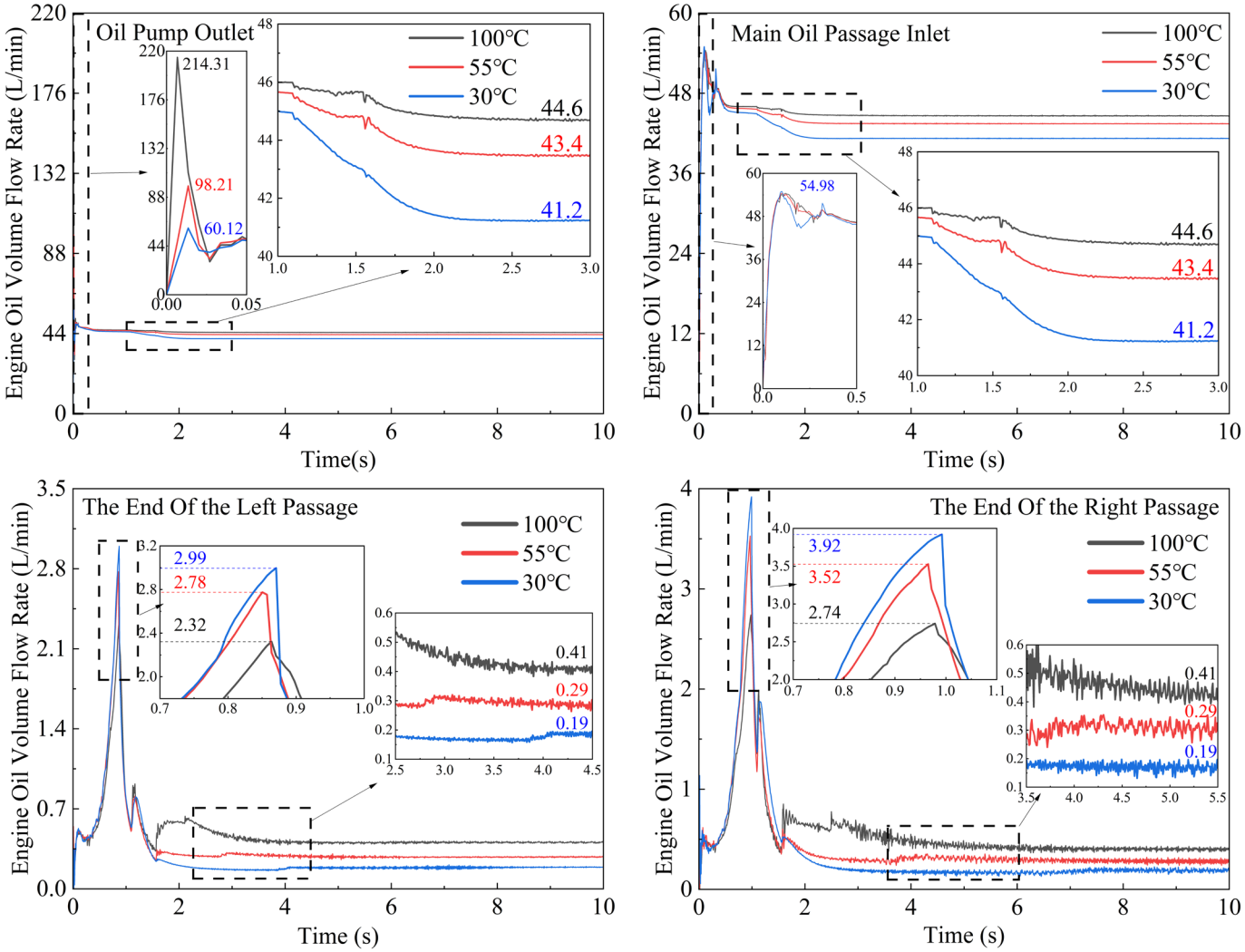


Figure 10. The influence of different oil temperatures on the oil volume flow rate at each node.

When the oil temperature decreases from 100 °C to 30 °C, the peak oil flow rate at the downstream end of the left main oil gallery increases from 2.32 L/min to 2.99 L/min, corresponding to an increase of approximately 28.9%, while the steady-state oil flow rate decreases from 0.41 L/min to 0.19 L/min, representing a reduction of approximately 53.7%. Similarly, at the downstream end of the right main oil gallery, the peak oil flow rate increases from 2.74 L/min to 3.92 L/min, with an increase of approximately 30.1%, whereas the steady-state oil flow rate decreases from 0.43 L/min to 0.17 L/min, corresponding to a reduction of approximately 60.5%. This phenomenon arises because, at the initial stage of diesel engine startup, the oil pump speed increases rapidly, and the oil flow rate is predominantly governed by the pump. As the oil temperature decreases, the increase in oil viscosity leads to an enhancement in the volumetric efficiency of the oil pump [24], thereby increasing the peak oil flow rate at the downstream ends of the main oil galleries. The time required for the oil flow rates at the downstream ends of the left and right main oil galleries to reach steady state is also prolonged by approximately 16.7%, which is consistent with the delays observed at the oil pump outlet and the inlet of the main oil gallery. These

results further confirm the dominant role of oil temperature in governing the overall flow characteristics of the lubrication system during the diesel engine startup process.

Figure 11 presents the oil filling status of the lubrication system at 2 s of the engine startup at various oil temperatures. As shown in the figure, with decreasing oil temperature, the oil requires a longer time to fill the entire lubrication system during the startup process. This phenomenon is attributed to the increased flow resistance associated with higher oil viscosity at lower temperatures, which slows the oil transport along the lubrication passages. Furthermore, the final result indicates that the oil completely fills the fifth crankshaft main bearing at approximately 5.1 s, at an oil temperature of 100 °C. When the oil temperature is reduced to 55 °C and 30 °C, the fifth crankshaft main bearing is fully filled at approximately 7.3 s and 8.7 s, respectively. As the oil temperature decreases from 100 °C to 30 °C, the oil filling time is prolonged by approximately 70.6%.

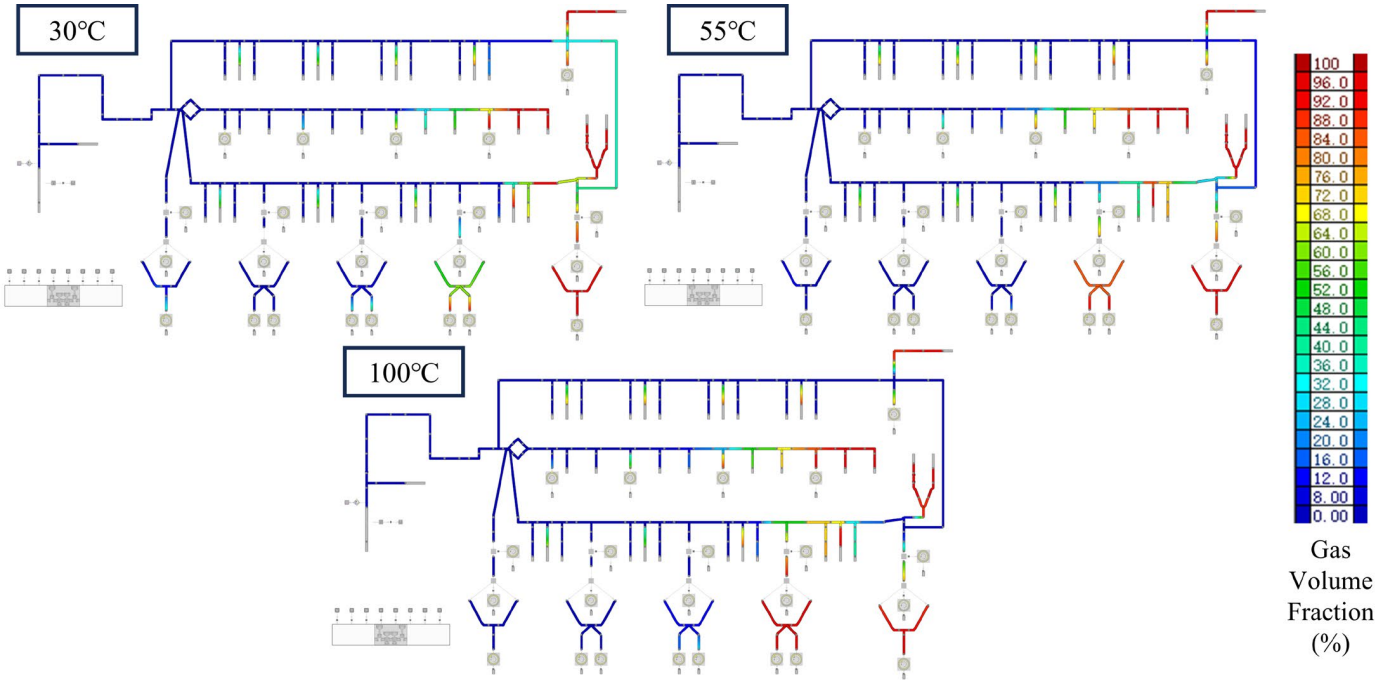


Figure 11. Oil filling status of the lubrication system at 2 s of the engine startup at various oil temperatures.

Figure 12 presents the calculated results of the minimum steady-state oil film thickness and the maximum steady-state oil film pressure of each main bearing under different oil temperature conditions. The results indicate that at an oil temperature of 30 °C, the steady-state minimum oil film thickness of the main bearings is approximately 10 μm, while the maximum oil film pressure is about 250 bar. When the temperature increases to 55 °C, the minimum oil film thickness decreases to approximately 7 μm, accompanied by an increase in the maximum oil film pressure to about 290 bar. As the temperature further rises to 100 °C, the minimum oil film thickness is significantly reduced to around 3 μm, whereas the maximum oil film pressure sharply increases to approximately 430 bar. Under this condition, the bearings are subjected to an elevated risk of boundary lubrication, making them more susceptible to severe wear. These results demonstrate that under high-altitude conditions, temperature reduction has a pronounced influence on bearing lubrication behavior: lower temperatures facilitate oil film formation and reduce oil film pressure, thereby improving the overall lubrication performance of the bearings.

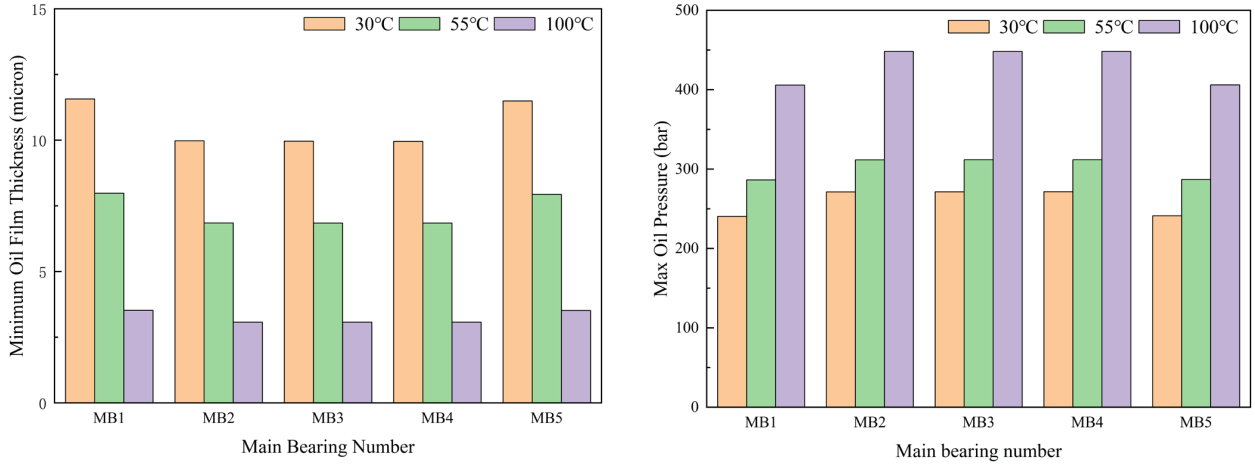


Figure 12. The lubrication status of each bearing: (**a**) maximum steady-state oil film pressure of each main bearing under different oil temperature conditions; (**b**) minimum steady-state oil film thickness of each main bearing under different oil temperature conditions.

3.3. Influence of Relief Valve Opening Degrees on the Startup Performance of Lubrication Systems

Figure 13 illustrates the transient oil pressure curves at the oil pump outlet, the inlet of the main oil gallery, and the downstream ends of the left and right main oil galleries under an ambient pressure of 0.88 bar for different opening degrees of the oil pump pressure relief valve. During the diesel engine cold-start process, as the opening degree of the oil pump pressure relief valve increases from the fully closed to the fully open condition, the steady-state oil pressure at the oil pump outlet decreases from 2.10 bar to 1.30 bar, corresponding to a reduction of 38.1%. The steady-state oil pressure at the inlet of the main oil gallery decreases from 1.69 bar to 1.15 bar, representing a reduction of 31.9%. At the downstream end of the left main oil gallery, the steady-state oil pressure decreases from 1.62 bar to 1.12 bar, with a reduction of 30.9%, while that at the downstream end of the right main oil gallery decreases from 1.61 bar to 1.12 bar, corresponding to a reduction of 30.4%.

The overall increase in oil pressure level during the startup process is reduced, which can be attributed to the decrease in oil leakage at the pump outlet due to the reduced opening of the pressure relief valve. In addition, as the opening degree of the oil pump pressure relief valve increases, a slight delay is observed in the time required for the oil pressure to reach its steady-state value.

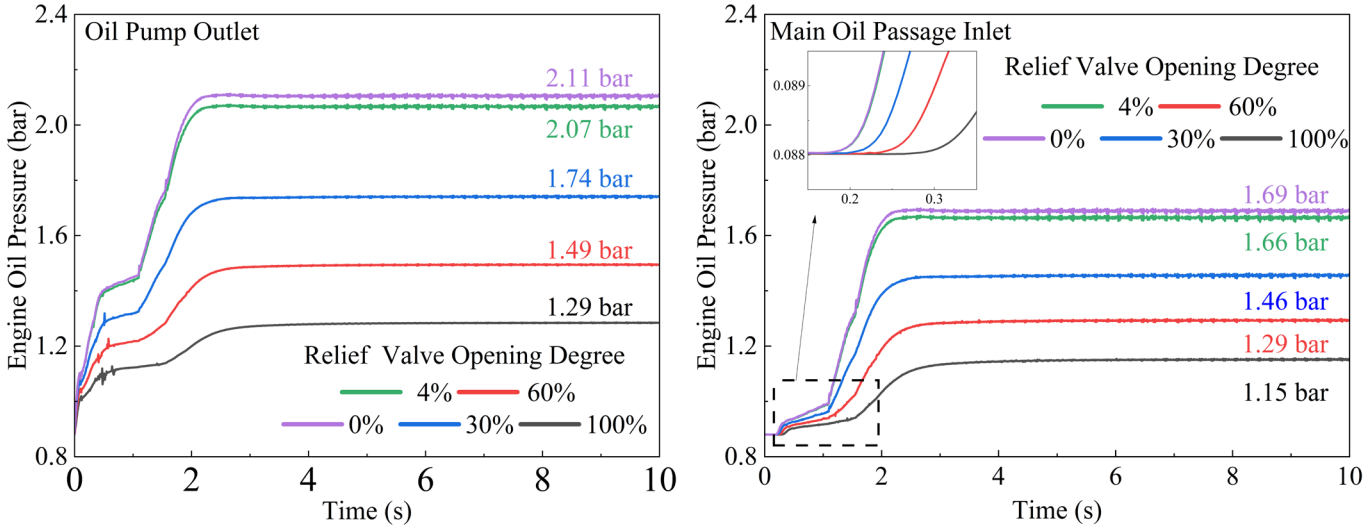


Figure 13. *Cont.*

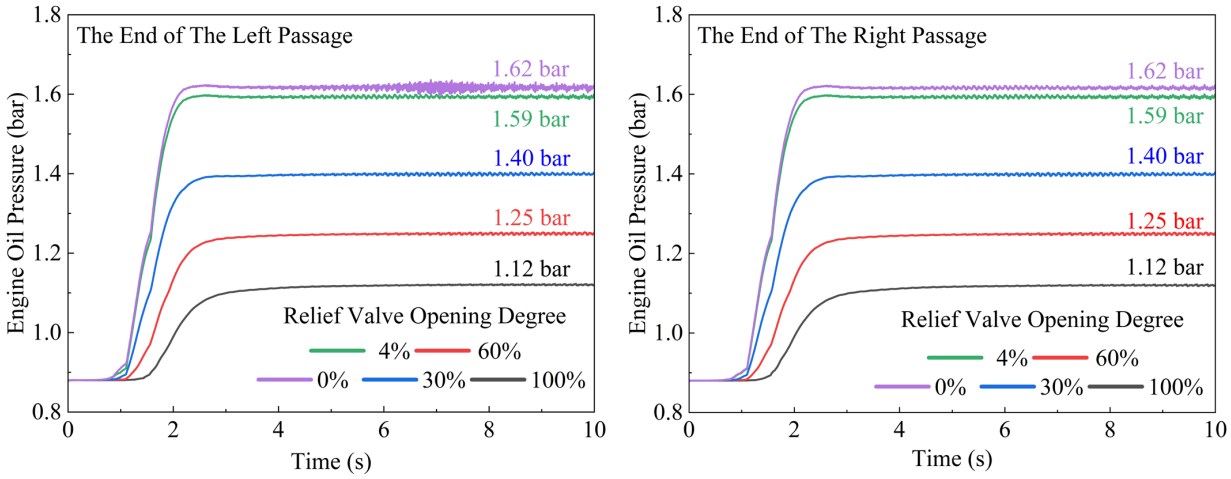


Figure 13. The influence of different relief valve opening degrees on the oil pressure at each node.

Under an ambient pressure of 0.88 bar, Figure 14 shows the transient oil flow rate curves at the oil pump outlet, the inlet of the main oil gallery, and the downstream ends of the left and right main oil galleries for different oil pump pressure relief valve openings. During the diesel engine startup process, as the opening of the oil pump pressure relief valve increases from fully closed to fully open, the steady-state oil flow rates at both the oil pump outlet and the inlet of the main oil gallery decrease from 42.3 L/min to 16.9 L/min, corresponding to a reduction of approximately 60%. In addition, the peak oil flow rates at these two key locations are also reduced, and the time required for the oil flow to reach a steady state is significantly prolonged.

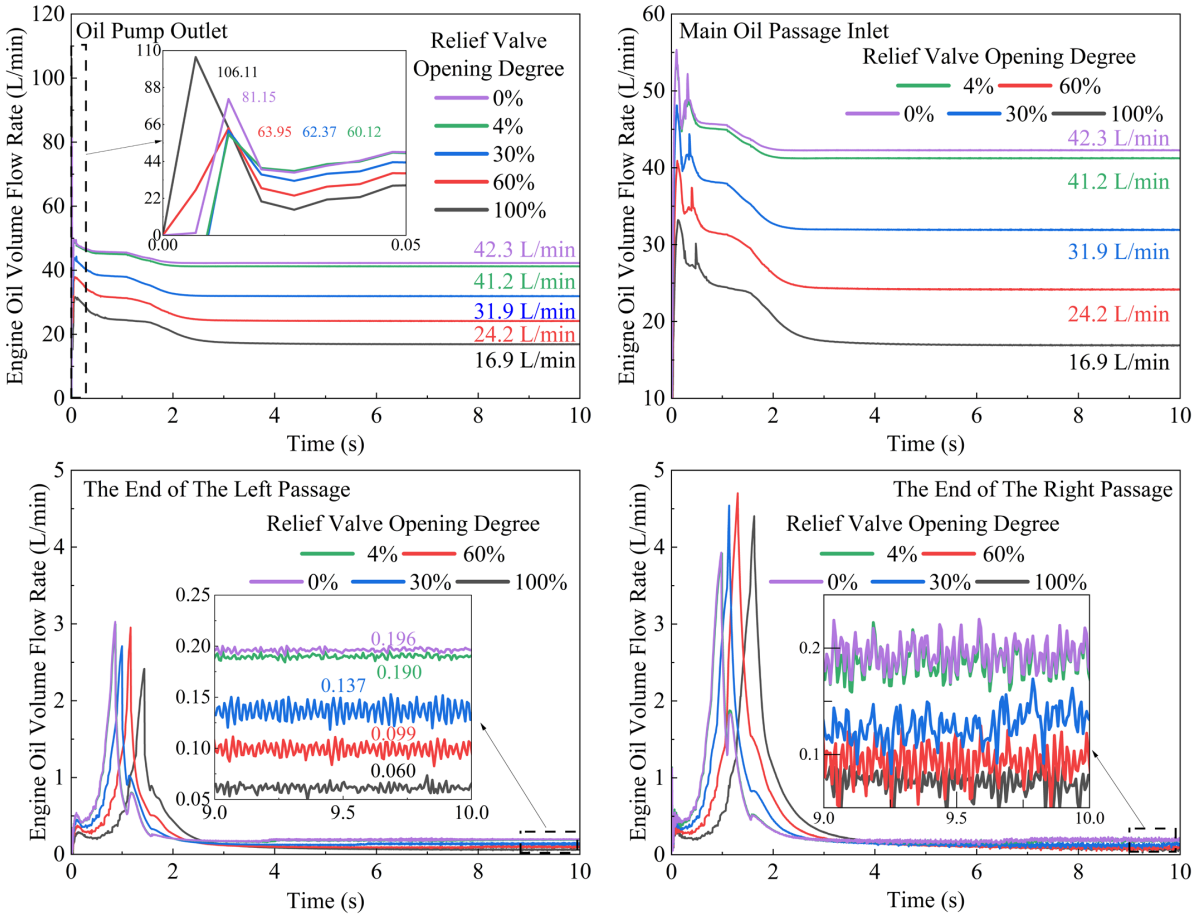


Figure 14. The influence of different relief valve opening degrees on the oil volume flow rate at each node.

In contrast, the steady-state oil flow rates at the downstream ends of the left and right main oil galleries exhibit only minor variations under different relief valve openings, with differences remaining within 0.2 L/min. However, as the relief valve opening increases, the time required for the oil flow at the downstream ends of the left and right main oil galleries to reach steady state increases markedly, following a trend similar to that observed at the oil pump outlet and the inlet of the main oil gallery, with an increase of approximately 19%.

Figure 15 presents the oil filling status of the lubrication system at 2 s of the engine startup at various relief valve opening degrees. As shown in the figure, the opening degree of the oil pump pressure relief valve has a pronounced influence on the oil filling rate of the lubrication system during the startup process. As the relief valve opening increases from the fully closed state to the fully open state, the oil filling rate within the lubrication system decreases accordingly. Furthermore, the final result indicates that oil reaches and completely fills the fifth crankshaft main bearing at approximately 8.5 s, when the pressure relief valve is fully closed. In contrast, when the relief valve is fully open, oil fills the fifth crankshaft main bearing at approximately 15.4 s, indicating that the total oil filling time of the lubrication system is prolonged by 86.7%.

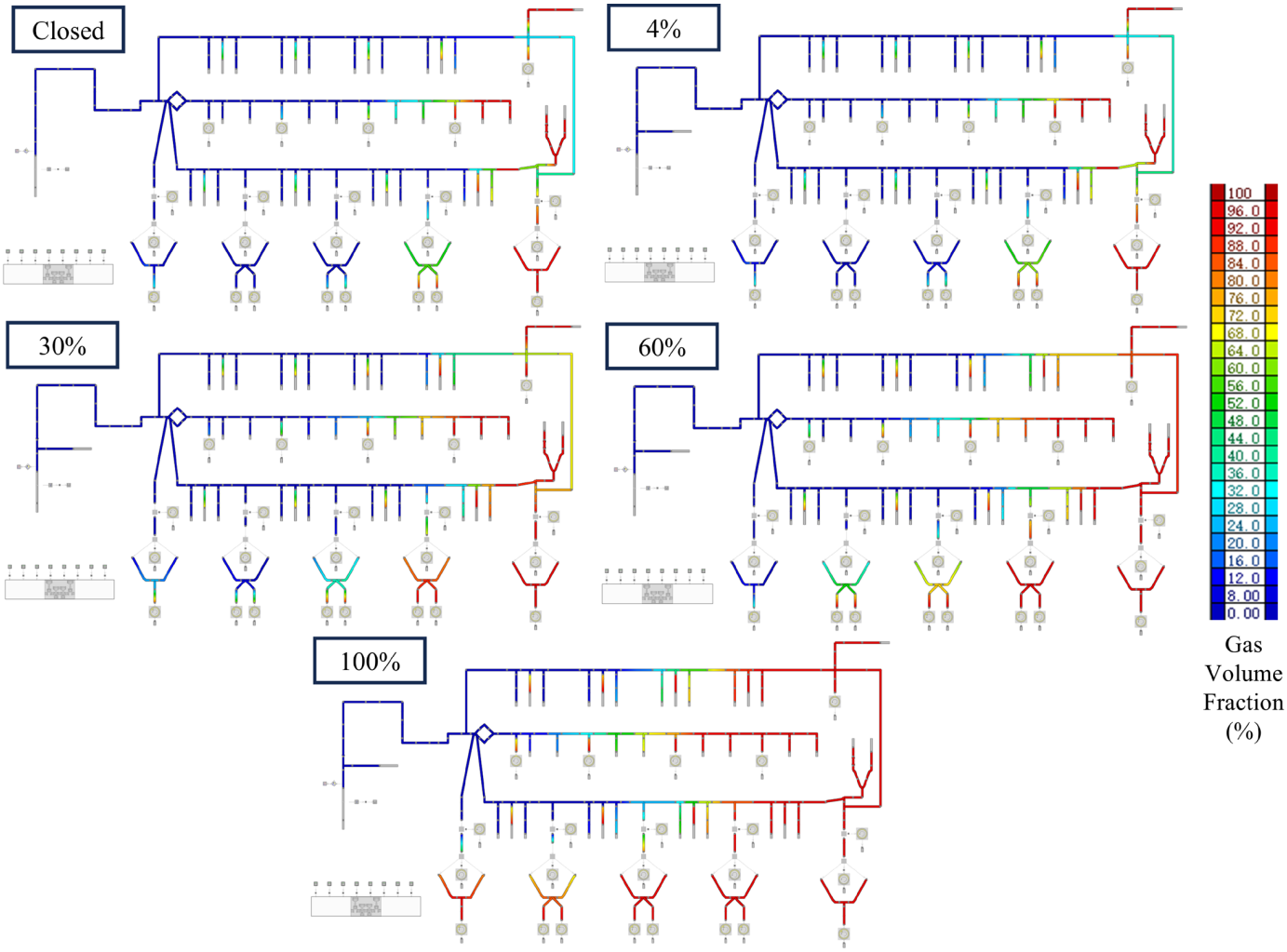


Figure 15. Oil filling status of the lubrication system at 2 s of the engine startup at various relief valve opening degrees.

Figure 16 presents the calculated minimum steady-state oil film thickness and maximum steady-state oil film pressure of each main bearing under different pressure relief valve opening conditions. The results indicate that the relief valve opening has only a

minor influence on bearing lubrication performance. As the valve opening increases, the minimum steady-state oil film thickness of the main bearings decreases from approximately 11.5 μm in the fully closed state to about 10 μm when fully open, while the maximum oil film pressure increases from 250 bar to 270 bar. These findings suggest that, under high-altitude conditions, an increase in the oil pump outlet relief valve opening slightly elevates the risk of boundary lubrication in the bearings; however, the overall effect remains limited.

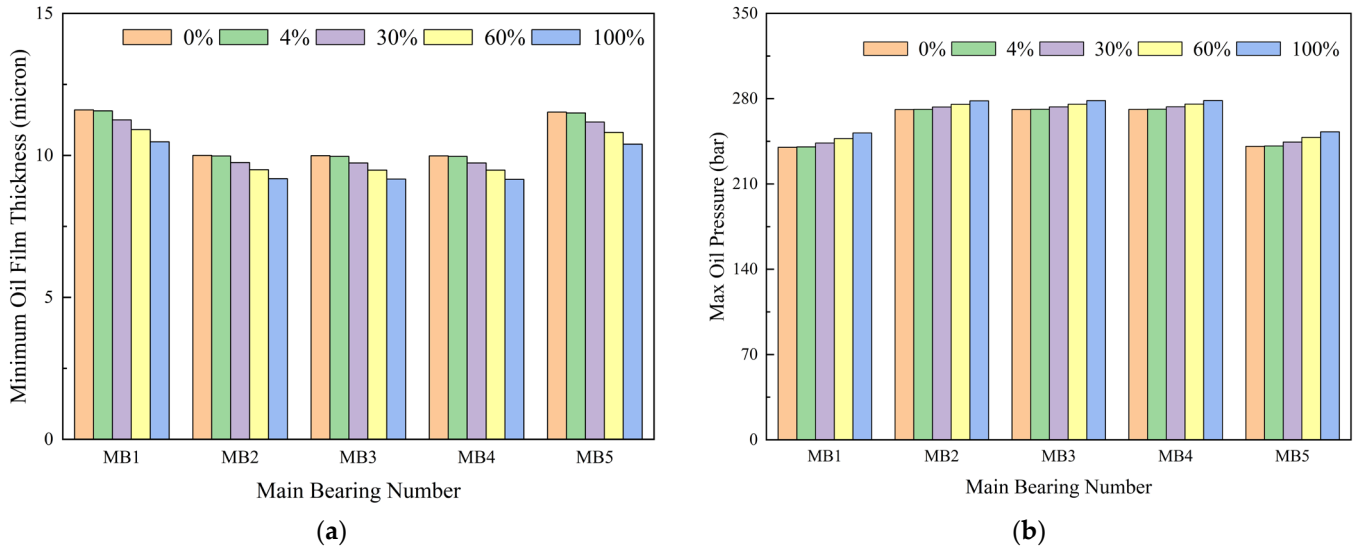


Figure 16. The lubrication status of each bearing: (**a**) maximum steady-state oil film pressure of each main bearing under different opening degrees of the pressure relief valves; (**b**) minimum steady-state oil film thickness of each main bearing under different opening degrees of the pressure relief valves.

4. Conclusions

To investigate the influence mechanisms of high-altitude and cold environments on the startup process of high-power diesel engine lubrication systems, a one-dimensional simulation model of the overall lubrication system was developed based on a physical experimental prototype. Three key variables—ambient pressure, oil temperature, and the opening degree of the oil pump pressure relief valve—were introduced to evaluate the direct effects of high-altitude and low-temperature environments on the startup behavior of the lubrication system. Based on the analysis of the simulation results, the following conclusions can be drawn:

(1) Variations in ambient pressure primarily cause a uniform shift in the absolute oil pressure level, without significantly affecting relative oil pressure, steady-state flow rate, response time, or oil filling rate. Its main role lies in lowering the absolute pressure boundary, thereby providing a quantifiable environmental parameter for friction pair reliability design and safety threshold calibration. Nevertheless, under the extrapolation assumption of the MAP of engine oil pump flow rate-pressure rise-rotating speed, there is a statistically significant correlation between the decrease in environmental pressure and a 24.5% reduction in the peak flow rate at the pump outlet. It provides a calculable early-warning threshold and experimental targeting basis for the lubrication reliability design of plateau engines.

(2) The pressure relief valve opening exerts a strong nonlinear influence on lubrication performance, especially on the oil filling process. Increasing the valve opening from fully closed to fully open prolongs oil filling time by 81.2% and reduces steady-state oil pressures throughout the system by approximately 30–38%. Flow rates at the oil pump outlet and main gallery inlet decrease by 60%, while downstream gallery flow remains nearly constant, with a 19% increase in response time. These results indicate that relief valve opening serves

as a critical intermediate factor that aggravates lubrication degradation under high-altitude and low-temperature conditions by increasing internal leakage. This result can serve as an important intervention target for high-altitude reliability design.

(3) Comparative results show that oil temperature is the dominant factor affecting startup lubrication under high-altitude conditions. A temperature reduction from 100 °C to 30 °C leads to nearly a 50% decrease in steady-state oil pressure and downstream flow rate, far exceeding the effects of reduced ambient pressure or increased relief valve opening. Overall, decreasing oil temperature has a substantially greater impact on lubrication performance than relief valve opening, while ambient pressure plays a comparatively minor role. This level of impact quantification provides a crucial basis for making design priority decisions.

Author Contributions: Conceptualization, H.Z. and W.D.; methodology, Y.G. and W.Z.; validation, Z.G. and L.H.; formal analysis, H.Z.; investigation, W.Z.; resources, L.H. and W.D.; data curation, Z.G.; writing-original draft preparation, Z.G.; visualization, H.Z.; supervision, Z.G. and Y.G.; project administration, H.Z. and L.H.; funding acquisition, L.H. and H.Z. All authors have read and agreed to the published version of the manuscript.

Funding: This research was funded by Hebei Natural Science Foundation [grant number E2024105055] and National Natural Science Foundation of China [grant number 52306038].

Data Availability Statement: Data are contained within the article.

Conflicts of Interest: Author Lanjie Huang was employed by the company Hebei Huabei Diesel Engine Co., Ltd. The remaining authors declare that the research was conducted in the absence of any commercial or financial relationships that could be construed as a potential conflict of interest.

References

1. Xu, H.; Liu, S.; Yin, B.; Jia, H.; Yu, S. Visualization of combustion performance and emission characteristics of a four-cylinder diesel engine at various inlet oxygen concentrations at part loads. *J. Mech. Sci. Technol.* **2018**, *32*, 2925–2934. [CrossRef]
2. Piqueras, P.; Burke, R.; Sanchis, E.J.; Diesel, B. Fuel efficiency optimisation based on boosting control of the particulate filter active regeneration at high driving altitude. *Fuel* **2022**, *319*, 123734. [CrossRef]
3. Varella, R.A.; Giechaskiel, B.; Sousa, L.; Duarte, G. Comparison of Portable Emissions Measurement Systems (PEMS) with Laboratory Grade Equipment. *Appl. Sci.* **2018**, *8*, 1633. [CrossRef]
4. Stepien, Z.; Urzedowska, W.; Oleksiak, S.; Czerwinski, J. Research on Emissions and Engine Lube Oil Deterioration of Diesel Engines with BioFuels (RME). *SAE Int. J. Fuels Lubr.* **2011**, *4*, 125–138. [CrossRef]
5. Rychtář, V.; Malý, M.; Zvolský, T. *Analysis of Dynamic Phenomena in the Hydraulic Circuit of the Engine Lubrication System*; Springer Nature: Cham, Switzerland, 2025; pp. 521–531.
6. Gambhir, A.; Tse, L.K.C.; Tong, D.; Martinez-Botas, R. Reducing China's road transport sector CO_2 emissions to 2050: Technologies, costs and decomposition analysis. *Appl. Energy* **2015**, *157*, 905–917. [CrossRef]
7. Hou, L.; Wang, Y.; Zheng, Y.; Zhang, A. The Impact of Vehicle Ownership on Carbon Emissions in the Transportation Sector. *Sustainability* **2022**, *14*, 12657. [CrossRef]
8. Zhang, H.; Zhu, W.; Guo, Y.; Du, W.; Yang, X.; Mei, B. Study on low temperature starting strategy for high power density diesel engines. *Proc. Inst. Mech. Eng. Part D J. Automob. Eng.* **2023**, *239*, 665–679. [CrossRef]
9. Chen, R.; Zhao, B.; Tu, L.; Xie, Z.; Lu, X.; Zou, D. Modelling and theoretical research on transient lubrication and wear coupling behavior of main bearing during start-up of low-speed diesel engine. *Proc. Inst. Mech. Eng. Part J J. Eng. Tribol.* **2024**, *239*, 480–498. [CrossRef]
10. Celik, A.; Yilmaz, M.; Yildiz, O.F. Effects of vortex tube on exhaust emissions during cold start of diesel engines. *Appl. Energy Combust. Sci.* **2021**, *6*, 100027. [CrossRef]
11. Yang, L.; Lei, J.; Wang, Z.; Wang, D.; Chen, J.; Li, D.; Liu, K.; Sun, L. Impacts of different ambient temperatures on cold-start characteristics of speed-up duration of an ISAD hybrid diesel engine in plateau. *Fuel* **2025**, *381*, 133492. [CrossRef]
12. Lu, K.; Qiu, H.; Chen, Z.; Shi, L.; Deng, K. Environmental adaptability method for improving the cold start performance of the diesel engine based on pilot injection strategy. *Energy* **2023**, *281*, 128215. [CrossRef]
13. Liu, J.; Li, Y.; Zhang, C.; Liu, Z. The effect of high altitude environment on diesel engine performance: Comparison of engine operations in Hangzhou, Kunming and Lhasa cities. *Chemosphere* **2022**, *309*, 136621. [CrossRef] [PubMed]

14. Zare, A.; Bodisco, T.A.; Verma, P.; Jafari, M.; Babaie, M.; Yang, L.; Rahman, M.M.; Banks, A.; Ristovski, Z.D.; Brown, R.J.; et al. Emissions and performance with diesel and waste lubricating oil: A fundamental study into cold start operation with a special focus on particle number size distribution. *Energy Convers. Manag.* **2020**, *209*, 112604. [CrossRef]
15. He, C.; Ge, Y.; Ma, C.; Tan, J.; Liu, Z.; Wang, C.; Yu, L.; Ding, Y. Emission characteristics of a heavy-duty diesel engine at simulated high altitudes. *Sci. Total Environ.* **2011**, *409*, 3138–3143. [CrossRef]
16. Ceballos, J.J.; Melgar, A.; Tinaut, F.V. Influence of Environmental Changes Due to Altitude on Performance, Fuel Consumption and Emissions of a Naturally Aspirated Diesel Engine. *Energies* **2021**, *14*, 5346. [CrossRef]
17. Qi, Z.; Gu, M.; Cao, J.; Zhang, Z.; You, C.; Zhan, Y.; Ma, Z.; Huang, W. The Effects of Varying Altitudes on the Rates of Emissions from Diesel and Gasoline Vehicles Using a Portable Emission Measurement System. *Atmosphere* **2023**, *14*, 1739. [CrossRef]
18. Meng, Z.; Liu, Z.; Liu, J. Investigation of in-cylinder combustion deterioration of diesel engines in plateau regions. *Fuel* **2022**, *324*, 124824. [CrossRef]
19. Garcia Tobar, M.; Cabrera Ojeda, O.; Crespo Montaño, F. Impact of Oil Viscosity on Emissions and Fuel Efficiency at High Altitudes: A Response Surface Methodology Analysis. *Lubricants* **2024**, *12*, 277. [CrossRef]
20. Keszthelyi, G.; Schmidt, J.; Denecke, J. Evaluation of one-dimensional models to predict chatter in spring-loaded pressure relief valves for gas service. *Process Saf. Environ. Prot.* **2024**, *182*, 1097–1109. [CrossRef]
21. Yang, L.; Wang, Z.; Dempster, W.; Yu, X.; Tu, S.-T. Experiments and transient simulation on spring-loaded pressure relief valve under high temperature and high pressure steam conditions. *J. Loss Prev. Process Ind.* **2017**, *45*, 133–146. [CrossRef]
22. Morselli, S.; Gessi, S.; Marani, P.; Martelli, M.; De Hieronymis, C.M.R. Dynamics of pilot operated pressure relief valves subjected to fast hydraulic transient. *AIP Conf. Proc.* **2019**, *2191*, 020116.
23. Okada, M.; Kawashima, S. On the equations of one-dimensional motion of compressible viscous fluids. *J. Math. Kyoto Univ.* **1983**, *23*, 55–71. [CrossRef]
24. Tan, Z.; Yang, T.; Zhao, H.; Zou, Q. Global Solutions to the One-Dimensional Compressible Navier–Stokes–Poisson Equations with Large Data. *SIAM J. Math. Anal.* **2013**, *45*, 547–571. [CrossRef]
25. Mellet, A.; Vasseur, A. Existence and Uniqueness of Global Strong Solutions for One-Dimensional Compressible Navier–Stokes Equations. *SIAM J. Math. Anal.* **2008**, *39*, 1344–1365. [CrossRef]
26. Liu, H.; Jurkschat, T.; Lohner, T.; Stahl, K. Detailed Investigations on the Oil Flow in Dip-Lubricated Gearboxes by the Finite Volume CFD Method. *Lubricants* **2018**, *6*, 47. [CrossRef]
27. Gao, W.; Li, C.; Li, Y.; Liu, Z.; Lyu, Y. Oil–Air Two-Phase Flow Distribution Characteristics inside Cylindrical Roller Bearing with Under-Race Lubrication. *Lubricants* **2024**, *12*, 133. [CrossRef]
28. Guo, Y.; Zhu, W.; Niu, P.; Gao, Z.; Yang, X.; Zhang, H. Mechanistic Effects of Prelubrication and Lubricant Preheating on Lubrication and Wear in Diesel Engines During Subzero Cold Starts. *J. Tribol.* **2025**, *148*, 012203. [CrossRef]
29. Inaguma, Y.; Yoshida, N. Mathematical Analysis of Influence of Oil Temperature on Efficiencies in Hydraulic Pumps for Automatic Transmissions. *SAE Int. J. Passeng. Cars-Mech. Syst.* **2013**, *6*, 786–797. [CrossRef]
30. Shen, M.; Zhang, F.; Liu, Y.; Zhou, X. Molecular dynamics study on the viscosity of hydraulic oil in the deep-sea environment. *J. Mol. Liq.* **2024**, *411*, 125716. [CrossRef]

Disclaimer/Publisher's Note: The statements, opinions and data contained in all publications are solely those of the individual author(s) and contributor(s) and not of MDPI and/or the editor(s). MDPI and/or the editor(s) disclaim responsibility for any injury to people or property resulting from any ideas, methods, instructions or products referred to in the content.